Platform Technologies for Minimally Invasive Physiological Monitoring

Mingui Sun[1,2,3,4], Steven A. Hackworth[1,2,4], Zhide Tang[1], Jun Zhao[1,4], Daliang L. Li[1,2,4]
Sharon E. Enos[4], Brian Errigo[4], Gary Gilbert[2,5], Ronald Marchessault[5]
Sylvain Cardin[5], Troy Turner[5], and Robert J. Sclabassi[1,2,3,4]

Laboratory of Computational Neuroscience
Departments of [1]Neurosurgery, [2]Electrical Engineering, and [3]Bioengineering
University of Pittsburgh, Pittsburgh, PA 15260
[4]Computational Diagnostics, Inc., Pittsburgh, PA 15213
[5]Telemedicine and Advanced Technology Research Center (TATRC)
US Army Medical Research & Materiel Command (USAMRMC)
Fort Detric, Frederick MD 21702

Abstract

Two critical problems exist in the engineering design of minimally invasive implantable devices: power supply and communication. Without solving these two problems, implantable devices will not be able to exchange information with the outside world and operate for extended periods of time. Currently, there exist only limited approaches to these problems. Inspired by the power delivery mechanisms of electric fish, we have developed a bio-mimetic approach using the volume conduction property of biological tissue as a natural cable to pass both information and power. A miniature device, called an energy pad, is designed. This device can be easily attached to the exterior of the skin for the purposes of communication and recharging of an implanted battery within the human body. The volume conduction system is analyzed by a linear network model and experimentally evaluated using samples of pig skin.

1 Introduction

For some time the military medical services have focused research on non-invasive physiological monitoring sensors as a means of obtaining data for remote triage of combat casualties and for soldier health and performance monitoring. It has become increasingly evident that, due to the lack of direct access to organ systems, non-invasive sensors may not be able to collect all the data parameters crucial to remote triage or soldier health status monitoring and prediction. Therefore invasive/internal physiological sensors may be needed. Potential battlefield applications of these devices include: 1) performing invasive physiological monitoring with biological sensors intended to provide data for assessing health status of soldiers or performing computer aided remote triage of combat casualties, 2) releasing computer selected protective drugs internally when a soldier is wounded or attacked by chemical/biological agents, 3) increasing the awareness of hostile environments by channeling sensor/computer generated signals directly to the human nervous system (brain-computer interface), and 4) enhancing human performance or vigilance at critical moments during a combat mission or rescue process by internal stimulation.

In recent years, there have been significant advances in computer-guided, minimally invasive surgery which enables rapid implantation/removal of miniature prosthetic or monitoring devices into/from the human body with little pain and complications. Thus, the implantation of millimeter or sub-millimeter sized devices within the human body has become increasingly feasible. In order to construct these devices and utilize them in a wide variety of military and civilian applications, platform technologies that common to essentially all implantable devices must be developed.

We have identified two critical platform technologies in the engineering design of the future minimally invasive implantable devices: power supply and communication. These two functions often share the same transmission channel, such as a transcutaneous cable connection chan-

Report Documentation Page

Form Approved
OMB No. 0704-0188

1. REPORT DATE **01 NOV 2006**	2. REPORT TYPE **N/A**	3. DATES COVERED **-**

4. TITLE AND SUBTITLE **Platform Technologies for Minimally Invasive Physiological Monitoring**	5a. CONTRACT NUMBER
	5b. GRANT NUMBER
	5c. PROGRAM ELEMENT NUMBER
6. AUTHOR(S)	5d. PROJECT NUMBER
	5e. TASK NUMBER
	5f. WORK UNIT NUMBER
7. PERFORMING ORGANIZATION NAME(S) AND ADDRESS(ES) **Laboratory of Computational Neuroscience Departments of Neurosurgery University of Pittsburgh, Pittsburgh, PA 15260**	8. PERFORMING ORGANIZATION REPORT NUMBER
9. SPONSORING/MONITORING AGENCY NAME(S) AND ADDRESS(ES)	10. SPONSOR/MONITOR'S ACRONYM(S)
	11. SPONSOR/MONITOR'S REPORT NUMBER(S)

12. DISTRIBUTION/AVAILABILITY STATEMENT
Approved for public release, distribution unlimited

13. SUPPLEMENTARY NOTES
See also ADM002075., The original document contains color images.

14. ABSTRACT

15. SUBJECT TERMS

16. SECURITY CLASSIFICATION OF:			17. LIMITATION OF ABSTRACT	18. NUMBER OF PAGES	19a. NAME OF RESPONSIBLE PERSON
a. REPORT **unclassified**	b. ABSTRACT **unclassified**	c. THIS PAGE **unclassified**	**UU**	**8**	

nel or a magnetic inductive coupling channel [1, 2, 3, 4]. Therefore, power supply and communication have been considered twin problems and studied simultaneously. In most cases, the performance of communication is closely related to the amount of available power supply the communication system usually consumes a significant portion of the total energy available to the device. Lack of adequate energy directly causes decreased performance, including short communication range, poor signal quality, and low data rates.

Although communication and power supply are crucial, systematic investigations on these two platform technologies are currently insufficient. Only limited options are available. Most commercial implantable devices, such as the pacemaker and deep brain stimulation (DBS) device, utilize a non-rechargeable battery which stores a sufficient amount of energy to allow the device to operate for several years. Because of the energy capacity requirement, the battery must be large and heavy. For example, the DBS device manufactured by Medtronic has a weight of 48 grams and a volume of 15.8 cm^3. Although the DBS device produces stimulation signals to be delivered to the deep region within the brain, there is no suitable location in the head where such a large and heavy device can be placed. As a result, the DBS device is surgically implanted within the chest just below the collar bone. A subcutaneous cabling harness is utilized to connect the device and the intracranial electrodes within the head. However, the long-distance subcutaneous connection within the body is problematic. Breakage of the cable, microfractures and migration of both the electrode and the leads due to the forces exerted by the movements of the patient, and faulty connectors between the electrodes and the extension wire have been documented in numerous cases[5]. It has been reported[6] that the hardware failure rate can be as high as 20% in initial use. These problems may require a re-operation to replace the wire harness. In certain cases, intracranial revision involving stereotactic retargeting must be performed.

The energy supply problem also contributes to the high cost of the implantable devices. In the DBS case, the battery is sealed within the implant so the entire device must be surgically replaced once the battery power is depleted. The period between repeated surgeries ranges from less than one year (heavy usage) to several years (normal usage). The combined costs of replacement device, accessories, and surgical procedures are approximately $25,000 for each replacement, perhaps the most expensive battery change in the world.

Besides the use of battery power, there exist two common methods for communication and energy supply. The first method uses a percutaneous interface in which a wire connection is made from a computer or dedicated hardware through the skin and connective tissue to the implanted device[7]. Most neural recording studies on animals have used wire connections, not because this is preferred, but because they facilitate system setup, avoid the unsolved technical problems of wireless telemetry, and allow the use of standard computers and off-the-shelf electronic components to obtain scientific data quickly at a low cost. Wire connections have also been utilized on human subjects for the evaluation of experimental neural implants, such as the well-known BrainGate experiment[8] where a pedestal (a percutaneous connector) links the external unit and the electrode array implanted on the motor cortex. Clearly, percutaneous designs are prone to infection and highly invasive. They can only be temporary in a well-controlled environment, not suitable for permanent use in outdoor settings, such as the battlefield.

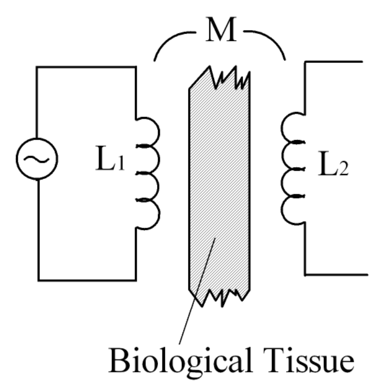

Figure 1: Magnetic inductive coupling

Another popular method for communication and power delivery is based on radio frequency (RF) magnetic inductive coupling where a transformer-like device consisting of a primary coil and a secondary coil is utilized (see Fig. 1). One of the coils is located inside the body while the other is located outside. When an RF signal is applied to the primary coil, current is induced in the secondary coil, through mutual inductance. Thorough treatments of the magnetic coupling technique are available and this technique has been applied to a number of implantable devices[2, 3]. However, this method has a major drawback. Its efficiency in power delivery is generally poor due to the energy loss in conductive biological tissue[9]. In addition, when an implant is small, which limits the size of the secondary coil, there is a rapid decline in magnetic flux captured by the secondary coil. In order to maintain a sufficient amount of power transfer, a large current must be delivered to the primary coil. This causes practical problems such as re-

quiring patients to carry an external battery at all times, an inconvenience in their daily life.

There exist several less common communication methods with implantable devices using antenna-based RF telemetry, a permanent magnet, optical coupling, and ultrasound coupling. These methods often suffer from excessive power drain from the power supply inside the implantable device and limited communication range.

We have been investigating a promising communication and power delivery method based on the volume conduction property of the human body. The ionic fluid in the biological body conducts electrical current which, when intentionally manipulated, is capable of transmitting information and power. This mechanism has been used to send data from the inside of a dolphin to a pair of remotely located electrodes placed in sea water[10], transmit information from a sensor implanted within a leg of a cadaver to perform mechanical measurements[11] and send information using a volume conduction body bus described in a recent Microsoft patent[12]. We have previously designed a volume conduction antenna which achieve a long communication range with a low power consumption[13]. We have also theoretically investigated the problem of bi-directional communication and shown that the volume conduction channel is symmetric[14]. In this work, we continue our investigation on communication and energy problems with emphasis on recharging neural implants for applications of invasive physiological monitoring and diagnosis. In these applications, the power requirement is usually moderate allowing an infrequent recharge of the battery inside the implanted device. We will present a new design of recharging system using a sticker-like device, called an energy pad, which can be conveniently pasted on the outside of the skin. This design was inspired by the energy delivery process of electric fish, which have a special organ emitting electric current into water to stun prey without bodily contact. We will also perform circuit analysis of the volume conduction system using linear 2-port network modeling. This paper will be concluded following a presentation of our experimental results using freshly harvested pig skin samples.

2 Methods

2.1 Bio-Inspired Energy Delivery

Although applying volume conduction based power delivery system to implantable devices is a new method, this mechanism already exists in nature where the electric eel, electric stingray, and other aquatic creatures deliver energy[15]. For example, the South American electric eel, a strongly electric fish, is capable of discharging 500V (head positive) at a maximum pulse frequency of 25Hz into its surrounding water through synchronized discharging of voltage generating cells known as electrocytes in the body[15, 16]. Weakly electric fish typically generates less than one volt in amplitude. Although the electric field of this type of fish cannot be used to stun prey, it can be used for navigation, object detection, and communication. It is interesting to observe that the weaponry organs of the strongly electric fish are arranged in a linear form. Each column of 5,000 to 10,000 electrocytes, connected in series, spans approximately 80% of the electric eels body. Approximately 70 columns are arranged in parallel on each side[16].

To simulate the discharge of the electric eel using finite element analysis, we approximated the electric eel in a top-down cross section and placed it in a cross-section of a large “fish tank. Our 2-D simulation results are shown in Fig. 2 where black curves and color both represent equal electric field strength, and arrows denote current density vectors whose length is proportional to the electric field strength. It can be observed that tail bending distorts the surrounding electric fields. Larger (smaller) fields are induced in the concave (convex) side. This indicates that the shape of the body helps to redistribute and focus electric energy.

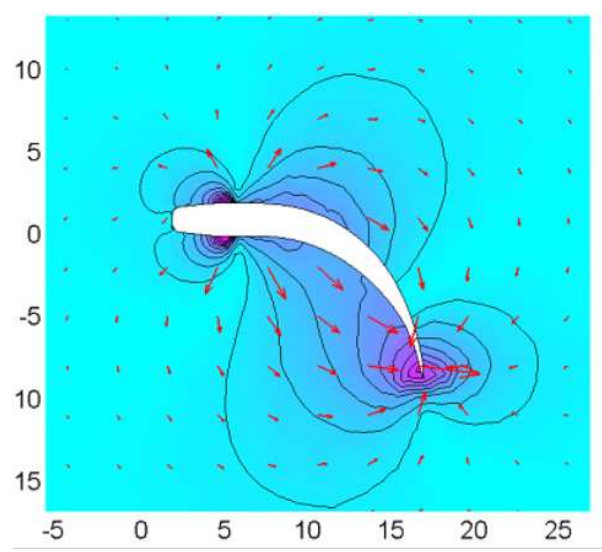

Figure 2: Simulated electric field of South American electric eel

The observed electrophysics of the electric fish inspired us to study the energy delivery problem using volume conduction. This mechanism is promising since nature has already provided us with an example of success. Using volume conduction has another attractive feature: it is a natural

resource available within our body since the biological tissue is admissive to electrical current of appropriate strength and frequency. The use of this resource therefore helps the implantable device to integrate with our biological system. In contrast, the RF is unnatural form of energy carrier because the ionic body fluids work against the RF signals, virtually preventing them from penetrating our system.

2.2 Energy Pad Design

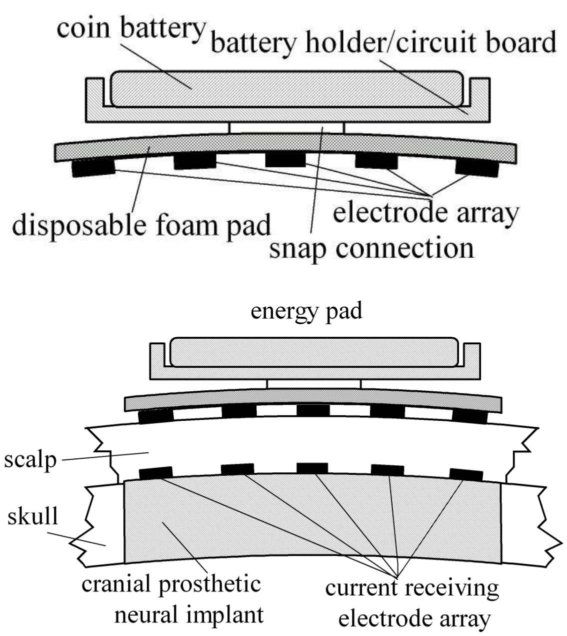

Figure 3: TOP: Fundamental design of energy pad; BOTTOM: Coupling between energy pad and implanted device

The energy pad, in the size of an American quarter, transmits energy and communication signals to an implanted device. The cross-sectional view of the energy pad is shown in Fig. 3. It consists of only three major components: a thin-profile button battery, a dual-use battery holder/circuit board, and a flexible foam pad. The functions of each component are described as follows. The battery, preferably a rechargeable lithium-ion (Li-ion) button battery, provides power to: 1) a DC/AC conversion and skin interface circuitry which delivers energy in an ionic current form to the implanted device within the human body, and 2) an electronic circuitry for communication, data acquisition, and control functions. The dual-use battery holder/circuit board, made of an insulating synthetic material, has the shape of a shallow baking pan. It not only holds the button battery, but also bears printed circuit patterns and SMT components on both sides which implement the energy conversion, communication, A/D and D/A, data storage, and control functions; The foam pad contains a signal/energy interface element, which transmits communication signals or energy to the implantable device (see the bottom panel in Fig. 3) in a similar fashion as the electric fish delivers current toward the target which, in our case, is the reception electrodes on the implanted device. A connector at the center of the foam electrically links the skin interface electrodes with the battery holder/circuit board. The foam pad, which is attached to the skin with adhesive similar to the ECG foam pad, conforms to the curvature of the body surface.

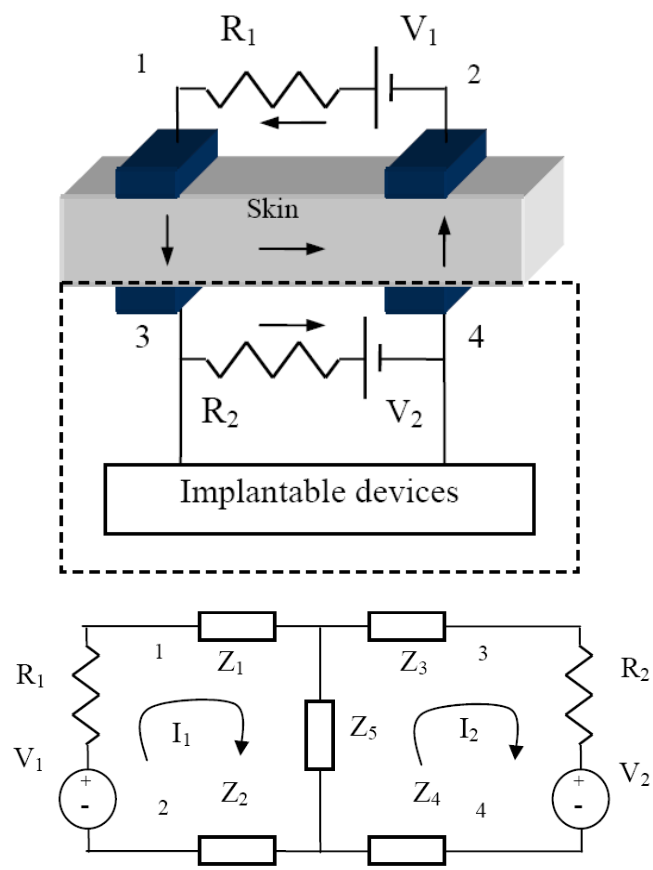

Figure 4: TOP: Simplified volume conduction system. The dashed box indicates the components within the implantable device; BOTTOM: Equivalent circuit model of the volume conduction system

3 System Analysis

In this section, we analytically study the mechanisms of energy delivery by the volume conduction system. In order to facilitate analysis, we simplify the original design

of the energy pad in Fig. 3 into the form shown in the top panel of Fig. 4. This electrode-skin unit consists of four electrodes (black blocks) and skin/connective tissue (gray block). The interior/exterior batteries and the equivalent series resistors (ESRs) are connected to electrodes. Note that, in practice, both the recharging and communication signals must be AC signals to reduce the effect of electrode polarization which takes place at the electrode-electrolyte interface[14, 17]. Therefore, the battery polarities shown in the bottom panel of Fig. 4 are instantaneous. Since the skin/connective tissue block represents a volume conductor, a complete characterization of the system requires numerically solving Poisson's equation (a partial differential equation) with a number of boundary conditions, which is computationally expensive. However, the volume conduction system can be considered passive and linear over the electrical ranges of interest and, for the study of current transmission through the four electrodes, the volume conduction system can be viewed as a "black box". Therefore, we modeled the system as a lumped, passive, and linear 2-port network. Our equivalent circuit model is shown in the bottom panel of Fig. 4. We call it the x-type equivalent circuit. Given the impedance values across the four electrodes, $Z_a = [Z_{12}, Z_{13}, Z_{14}, Z_{23}, Z_{24}, Z_{34}]$, the circuit parameters, $Z_b = [Z_1, Z_2, Z_3, Z_4, Z_5]$, can be calculated. From the equivalent circuit, we have

$$\begin{pmatrix} 1 & 1 & 0 & 0 & 1 \\ 1 & 0 & 1 & 0 & 0 \\ 1 & 0 & 0 & 1 & 1 \\ 0 & 1 & 1 & 0 & 1 \\ 0 & 1 & 0 & 1 & 0 \\ 0 & 0 & 1 & 1 & 1 \end{pmatrix} \begin{pmatrix} Z_1 \\ Z_2 \\ Z_3 \\ Z_4 \\ Z_5 \end{pmatrix} = \begin{pmatrix} Z_{12} \\ Z_{13} \\ Z_{14} \\ Z_{23} \\ Z_{24} \\ Z_{34} \end{pmatrix} \tag{1}$$

where the right-most vector contains the impedance values between pairs of electrodes (which are numbered in the top panel of Fig. 4), and the following constraint applies:

$$Z_{12} + Z_{34} - Z_{14} - Z_{23} = 0 \tag{2}$$

Based on the assumed current directions of I_1 and I_2 in Fig. 4, the following loop current equations can be obtained:

$$\begin{pmatrix} R_1 + Z_1 + Z_2 + Z_5 & -Z_5 \\ -Z_5 & R_2 + Z_3 + Z_4 + Z_5 \end{pmatrix} \begin{pmatrix} I_1 \\ I_2 \end{pmatrix} = \begin{pmatrix} V_1 \\ -V_2 \end{pmatrix} \tag{3}$$

From (3), the current transmission efficiency, defined as the ratio between the amplitude values of the received current I_2 and the emitted current I_1 can be calculated as

$$\eta_I = \left|\frac{I_2}{I_1}\right| = \left|\frac{1 - \frac{R_1+Z_1+Z_2+Z_5}{Z_5}\frac{V_2}{V1}}{\frac{R_2+Z_3+Z_4+Z_5}{Z_5} - \frac{V_2}{V_1}}\right|. \tag{4}$$

Using the equivalent circuit, it can be similarly shown that, for recharging to take place, the following condition must be satisfied:

$$\frac{V_{1m}}{V_2} > \left|\frac{R_1 + Z_1 + Z_2 + Z_5}{Z_5}\right| > 1. \tag{5}$$

where V_{1m} is the maximum voltage amplitude of the external power Source. From Eq. (5), The following features can be observed: 1) for recharging to take place, the maximum amplitude of the external voltage source must be higher than the voltage of the internal battery; and 2) the ESR of the internal battery does not affect the condition for recharging, but the ESR of the external voltage source does.

In order to make the recharging process effective, the current flowing through the internal battery must be sufficiently large. From Eq.(4), there are two approaches to increase the efficiency: 1) choosing circuit impedance parameters Z_1 through Z_5 to maximize the value of Eq.(4); and 2) increasing the voltage ratio $|\frac{V_1}{V_2}|$. The maximization process can be performed in three ways. First, electrode material can be selected to decrease the contact impedance with the skin. This selection affects Z_1 through Z_4 . Second, since the impedance of the human skin is a function of signal frequency[18], a proper selection of frequency can provide desirable permittivity and conductivity values. Finally, the geometric shapes and arrangements of electrodes can be optimized to affect Z_1 through Z_4.

The current transmission efficiency can also be raised by increasing $|\frac{V_1}{V_2}|$. However, V_2 is usually fixed due to the requirement of integrated circuit chips and V_1 is limited by the input current tolerance of the skin. From the circuit in the bottom panel of Fig. 4, when $|V_1| >> |V_2|$, the input current I_1 is given by

$$I_1 = \frac{V_1(Z_3 + Z_4 + Z_5)}{(Z_1 + Z_2 + Z_3 + Z_4)Z_5 + (Z_1 + Z_2)(Z_3 + Z_4)} \tag{6}$$

where the source ESRs are neglected. Given the maximum tolerable I_1 and the equivalent circuit impedances, the limit of the external voltage V_1 can be determined from Eq. (6).

4 Experimental Results

We have constructed a prototype circuit to recharge a 3V nominal battery via volume conduction. The block diagram of the recharging circuit is shown in Fig. 5. The DC/AC block converts the DC voltage to AC, exciting external electrodes 1 and 2. The AC signal is transmitted to the internal electrodes 3 and 4 through the volume conduction of the skin/tissue layer. Then, the AC/DC block rectifies the signal into a DC current which recharges the

internal battery. We used a lithium-ion battery (Panasonic, Type ML2020, voltage 3V, capacity 45mAh) for the internal battery which was drained to 1.9V before the experiments started. The DC/AC converter was replaced by a square wave generator and a power amplifier.

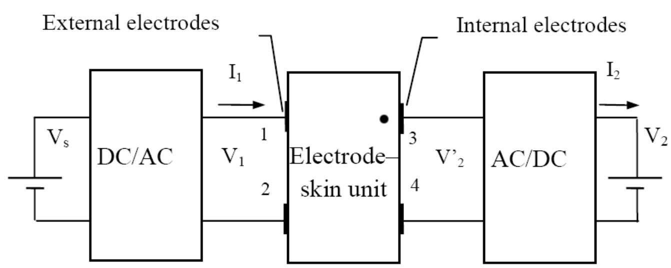

Figure 5: Block diagram of the experimental setup

4.1 Electrode-Skin Unit

The electrode-skin unit was the most important part of the recharging system. We used rectangular electrodes shown in the top panel of Fig. 6. The electrodes are made of copper and coated with tin. With an approval by the Institutional Animal Care and Use Committee, a small piece of freshly harvested pig skin (within 3 hours postmortem) was utilized in our experimental electrode-skin unit (see the bottom panel of Fig. 6).

4.2 AC Current Transmission of Electrode-Skin Unit

In order to verify our equivalent circuit model in Fig. 4, we examined AC current transmission through the actual electrode-skin unit. A sinusoidal voltage source of 1 kHz (with an ESR of 517 Ω) was applied between external electrodes 1 and 2, and a load (517 Ω) was connected between internal electrodes 3 and 4 of the electrode-skin unit. The measured current and the current transmission efficiency are shown in the top panel of Fig. 7. Then, we measured the impedance values between electrodes and established the equivalent circuit using (1). Finally, we calculated the current and current transmission efficiency values based on our equivalent circuit model. The results are shown in the bottom panel of Fig. 7. Clearly, these two plots are very similar which indicate that our circuit model is valid.

4.3 Waveforms of charging current

Since the current transmission efficiency increases as the voltage ratio V_1/V_2 increases, it can be hypothesized that the square wave charging current is more favorable than the sinusoidal wave. In order to test this hypothesis, sinusoidal and square wave voltage sources were applied to external electrodes 1 and 2 of the electrode-skin unit. The internal voltage was from the same lithium-ion battery mentioned previously. The charging signal frequency was 5 kHz. The root mean square value of the charging current I_2 was measured. A comparison of our results is shown in the top panel of Fig. 8, which indicates up to 13% larger charging current using the square wave than using the sinusoidal wave. This experiment validates the previous hypothesis.

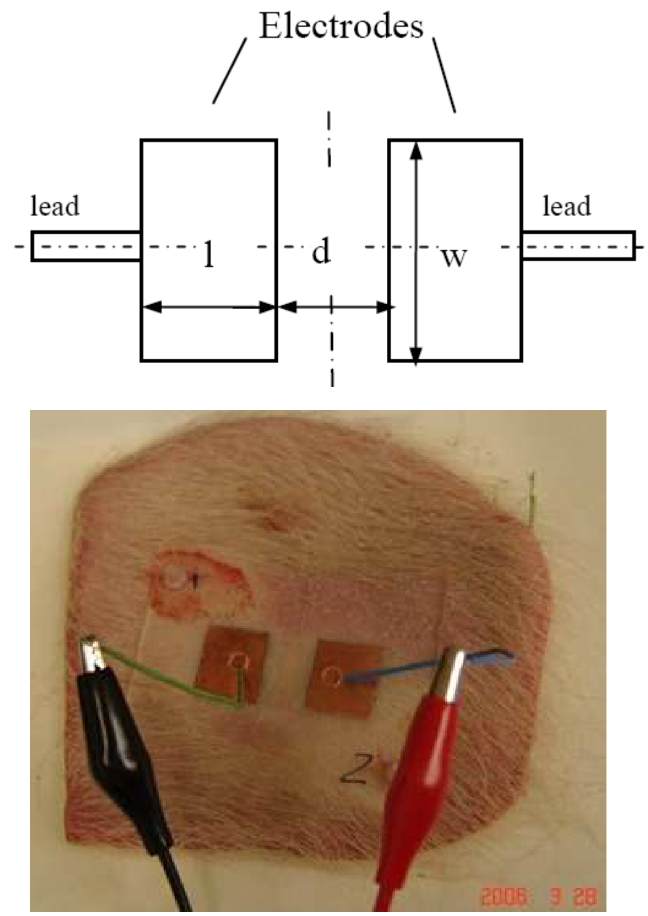

Figure 6: TOP: Electrode dimensions: $d = 5$mm, $w = 15$mm, and $l = 15$mm; BOTTOM: Electrode-skin unit using freshly harvested pig skin sample.

4.4 Frequency Selection

The impedance values, which include both the resistive and reactive parts, of biological tissues are functions of signal frequency. In order to select an appropriate frequency for the charging current, we conducted experiments where the current transmission efficiency values were measured. In these experiments, the amplitude of the external voltage

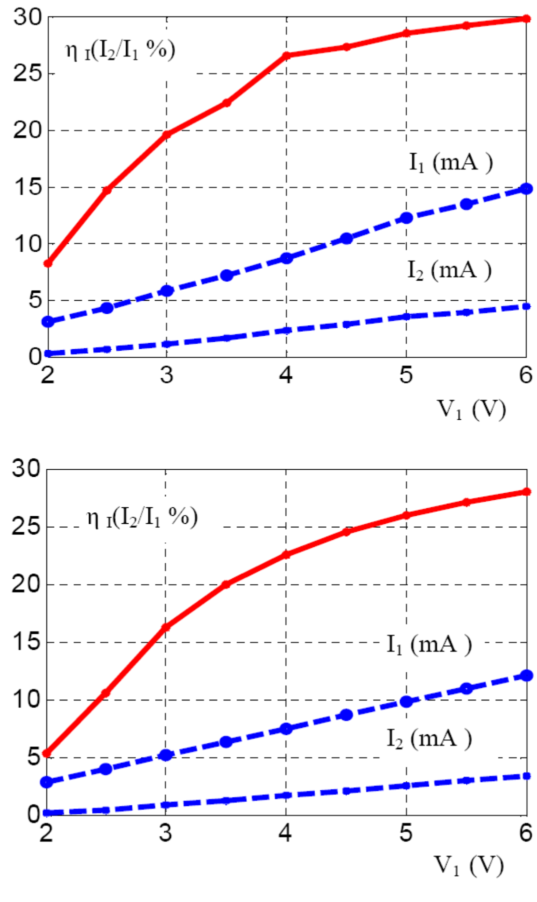

Figure 7: TOP: Experimentally measures current and efficiency values; BOTTOM: Calculated current and efficiency values using equivalent circuit model

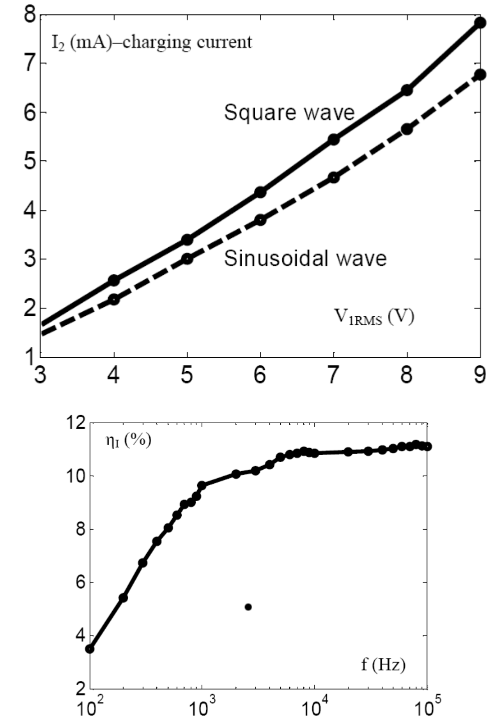

Figure 8: TOP: Charging current I_2 resulting from square and sinusoidal waves; BOTTOM: Current transmission efficiency $\eta_I = \frac{I_2}{I_1}$ vs. frequency f

source was kept constant at 5.7V while the frequency varied. The results are shown in the bottom panel of Fig. 8 where it can be observed that the current transmission efficiency increases rapidly at low frequencies, but reaches a plateau as the frequency increases further. It can also be observed that our choice of 5 kHz current is appropriate since a higher frequency does not produce a significant increase in efficiency.

5 Conclusion

In this work we have provided an effective solution to the communication and power supply problems with medical implants intended for soldier physiological monitoring, remote triage, and internal telemedical intervention. A practical design of an energy delivery system, inspired by the energy delivery mechanism of electric fish, is presented consisting of a simple and convenient external device called an energy pad. This small-size, light-weight device can be easily pasted on the skin at the time when the implanted device needs to be recharged. An AC current is delivered through the skin using the volume conduction property of the biological tissue. We have analytically studied this new design using a linear 2-port network model which provides a number of useful formulas for the optimal design of the volume conduction system. We have also constructed a test system using freshly harvested pig skin samples. Our experiments have validated our circuit model and shown that the square wave charging voltage is optimal and that the optimal selection of frequency for the charging current is in the kilohertz range.

Acknowledgments

This work was supported in part by US Army Medical Research and Materiel Command contract No. W81XWH-050C-0047, National Institutes of Health grant No. EB002099, and Computational Diagnostics, Inc.

Opinions, interpretations, conclusions, and recommendations expressed in this work are those of the authors and are not necessarily endorsed by the U.S. Army and other funding agencies. This research complies with the Animal

Welfare Act and the Guide for the Care and Use of Laboratory Animals.

References

[1] T. B. Hunter, M. T. Yoshino, R. B. Dzioba, R. A. Light, W. G. Berger, “Medical devices of the head, neck, and spine,” *Radiographics*, Jan-Feb 2004 24(1):257-85.

[2] W. Liu, M. Sivaprakasam, G. Wang, M. Zhou, J. Granacki, J. LaCoss, and J. Wills, “Implantable biomimetic microelectronic systems design,” *IEEE Engineering in Medicine and Biology Magazine*, Sept/Oct 2005, 24(5):66-74.

[3] W. J. Heetderks, “RF powering of millimeter- and submillimeter-sized neural prosthetic implants,” *IEEE Trans. Bioengineering*, 1998, 33:323-327.

[4] M. Ghovanloo, K. J. Otto, D. R. Kipke, and K. Najafi, “In vitro and in vivo testing of a wireless multichannel stimulating telemetry microsystem,” *Proc. IEEE Int. Conf. EMBS*, 2004, 4294-4297.

[5] D. Kondziolka, D. Whiting, A. Germanwala, M. Oh, “Hardware-related complications after placement of thalamic deep brain stimulator systems,” *Stereotact Funct Neurosurg.*, 2002, 79(3-4):228-33.

[6] C. Joint,D. Nandi, S. Parkin, R. Gregory, T. Aziz, “Hardware-related problems of deep brain stimulation,” *Mov Disord.*, 2002, 17 Suppl 3:S175-S180.

[7] L. Rucker, A. Lossinsky, “Percutaneous connectors,” *30th neural Prosthesis Workshop, NINDS, NINCD, NIH,* Oct 1999, 12-14.

[8] L.R. Hochberg, M.D. Serruya, G. M. Friehs, J. A. Mukand, M. Saleh, A. H. Caplan, A. Branner, D. Chen, R. D. Penn, and J. P. Donoghue, “Neuronal ensemble control of prosthetic devices by a human with tetraplegia. *Nature*, 2006, 442:164-171.

[9] A. J. Johansson, “Wireless Communication with Medical Implants: Antennas and Propagation,” *Faculty of Technology*, Lund University, Lund, Sweden, 2005.

[10] R. S. Mackay, *Bio-medical telemetry: sensing and transmitting biological information from animals and man*, Wiley, 2nd Ed., New York, 1998.

[11] E. L. McKee, D. P. Lindsey, M. L. Hull and S. M. Howell, “Telemetry system for monitoring anterior cruciate ligament graft forces in vivo,” *Med Biol Eng Comput.*, 1998, 36:330-336.

[12] L. Williams, *et al.* (Microsoft Corporation), *Method and apparatus for transmitting power and data using the human body*, U.S. Patent No. 6,754,472, Issue date: June, 2004.

[13] M. Sun, M. Mickle, W. Liang, Q. Liu, and R. J. Sclabassi, “ Data Communication between Brain Implants and Computer,” *IEEE Transactions on Neural Systems and Rehabilitation Engineering*, 2003, 11(2):189-192.

[14] M. Sun, Q. Liu, W. Liang, B. L. Wessel, P. A. Roche, M. Mickle, and R. J. Sclabassi, “Application of the Reciprocity Theorem to Volume Conduction Based Data Communication Systems between Implantable Devices and Computers,” *In IEEE Proc. EMBS’03*, Cancun, Mexico, 2003, 4:3352-3355.

[15] P. Moller, “Electric eel,” *in Electric Fishes*, 1995, pp. 400-402.

[16] M. V. L. Bennett, “Electric organs,” *in Fish Physiology*, Academic Press, London, 1971, V:347-491.

[17] J. G. Webster, *Medical Instrumentation: Application and Design, 3rd Edition*, Wiley, Hoboken, NJ.

[18] S. Grimnes and O.G.Martinsen, Bioimpedance & Bioeletricity Basics, San Diego, CA, Academic Press, 2000.